

# THE CIRCULANT MATRIX FORMALISM AND THE ROLE OF BEAM-BEAM EFFECTS IN COHERENT INSTABILITIES

X. Buffat, Geneva, Switzerland

## Abstract

The role of beam-beam interactions in coherent instabilities in high energy colliders is discussed with a particular emphasis on the circulant matrix model. This model, based on the development of a one-turn matrix including all linearised coherent forces, is particularly suited for the study of the stability of complex configurations involving different forces. Thus it allows for the study of interplays, e.g. between the effect of the beam-beam interactions and the beam coupling impedance. Experimental evidence compatible with this model is reported.

## INTRODUCTION

In a high energy collider, the stability of both beams needs to be considered in a common framework due to the electromagnetic interaction between the beams, that strongly couple their dynamics. In some configurations, the coherent beam-beam modes can be neglected and the effect of the beam-beam interaction on the beam stability is limited to its impact on the amplitude detuning and consequently on Landau damping [1, 2]. Here we focus on regimes where the models that consider the dynamic of the two beams separately, so-called weak-strong regimes, do not represent accurately the dynamics of the two beams. This applies to colliders where both beams feature a high brightness, i.e. most electron-positron or proton-proton colliders. We start by deriving the coherent force between the two beams. Based on this force, we introduce the rigid bunch model to obtain the coherent modes of oscillation in the most simplistic configuration and then extend this model to the circulant matrix model. Two methods used to make predictions beyond the linearised model are discussed. Finally, observations of coherent beam-beam modes showing the accuracy of the model are reported.

## THE COHERENT BEAM-BEAM FORCE

The beam-beam kick on a point-like particle, called the incoherent beam-beam kick, can be obtained by integration of Poisson's equation [3]. Using a Gaussian distribution of particles, with r.m.s. transverse beam size  $\sigma = \sigma_x = \sigma_y$ , one obtains the kick felt by a test particle at a position  $(x, y)$  with respect to the other beam's centroid [4] :

$$\Delta x' = -\frac{2r_0 N}{\gamma} \frac{x}{r^2} \left( 1 - e^{-\frac{r^2}{2\sigma^2}} \right), \quad (1)$$

where we have introduced  $N$  the number of charges in the beam,  $r_0$  the classical radius,  $r = \sqrt{x^2 + y^2}$  and the relativistic  $\gamma$  factor. Since the opposing beam is not point-like,

the total beam-beam kick, called coherent kick, is obtained by integration of the single particle kicks over the beam distribution  $\Psi(x, y)$  :

$$\Delta x'_{\text{coh}}(x, y) = \int_{-\infty}^{\infty} dX dY \Delta x'(X, Y) \Psi(X - x, Y - y). \quad (2)$$

Assuming a round Gaussian distribution and using Eqs. 1 and 2, we have [5] :

$$\Delta x'_{\text{coh}}(x, y) = -\frac{2r_0 N}{\gamma} \frac{x}{r^2} \left( 1 - e^{-\frac{r^2}{4\sigma^2}} \right). \quad (3)$$

For  $x, y \ll \sigma$ , we find that the coherent kick is half the single particle kick, whereas for large separation, i.e for long-range interactions, the difference between coherent and incoherent vanishes.

## THE RIGID BUNCH MODEL

In order to obtain a description of the coherent beam-beam modes, we want to solve the equations of motion of the two beams self-consistently. We use as dynamical variables the average transverse positions and momenta  $(x_l, x'_l)$  of the two beams ( $l = 1, 2$ ) with respect to their closed orbits assuming that their particle distribution remains Gaussian with fixed sizes in all degrees of freedom. By linearising all forces, we may derive the one-turn matrix of this periodic dynamical system and perform a normal mode analysis, including the beam-beam interactions self-consistently, thus describing the coherent modes of oscillation. Let us start by defining the one-turn matrix of a single beam with a transverse tune  $Q$  and using the optical  $\beta$  function at the interaction point  $\beta^*$  as  $M_{1B}$  giving its coordinate at turn  $k + 1$  with respect to the ones at turn  $k$  :

$$\begin{aligned} \begin{pmatrix} x_{l,k+1} \\ x'_{l,k+1} \end{pmatrix} &= \begin{pmatrix} \cos(2\pi Q) & \beta^* \sin(2\pi Q) \\ -\frac{1}{\beta^*} \sin(2\pi Q) & \cos(2\pi Q) \end{pmatrix} \cdot \begin{pmatrix} x_{l,k} \\ x'_{l,k} \end{pmatrix} \\ &\equiv M_{1B} \cdot \begin{pmatrix} x_{l,k} \\ x'_{l,k} \end{pmatrix}. \end{aligned} \quad (4)$$

For the two identical beams, we may define  $M_{2B}$  as the two-beam one-turn matrix :

$$\begin{pmatrix} x_{1,k+1} \\ x'_{1,k+1} \\ x_{2,k+1} \\ x'_{2,k+1} \end{pmatrix} = \mathbb{I}_2 \cdot M_{1B} \cdot \begin{pmatrix} x_{1,k} \\ x'_{1,k} \\ x_{2,k} \\ x'_{2,k} \end{pmatrix} \equiv M_{2B} \cdot \begin{pmatrix} x_{1,k} \\ x'_{1,k} \\ x_{2,k} \\ x'_{2,k} \end{pmatrix}, \quad (5)$$

with  $\mathbb{I}_n$  the identity matrix of size  $n$ . Within this basis, the matrix for a beam-beam interaction may be derived by

linearising Eq. (3) around  $(x_0, y_0)$  the closed orbit difference between the two beams at the interaction point :

$$\Delta x'_{\text{coh}}(x, y) \approx \Delta x'_{\text{coh}}(x_0, y_0) + \frac{\partial \Delta x'_{\text{coh}}}{\partial x}(x_0, y_0) \Delta x, \quad (6)$$

with :

$$\begin{aligned} \frac{\partial \Delta x'_{\text{coh}}}{\partial x}(x, y) = & -\frac{2Nr_0}{\gamma} \left[ \left( \frac{1}{r^2} - 2\frac{x^2}{r^4} \right) \left( 1 - e^{-\frac{r^2}{4\sigma^2}} \right) \right. \\ & \left. + \frac{x^2}{2r^2\sigma^2} e^{-\frac{r^2}{4\sigma^2}} \right]. \end{aligned} \quad (7)$$

Defining  $k_0 \equiv \frac{\partial \Delta x'_{\text{coh}}}{\partial x}(x_0, y_0)$ , one can then write the coupling matrix between the two beams, due to the beam-beam interaction :

$$M_{\text{BB}} = \begin{pmatrix} 1 & 0 & 0 & 0 \\ -k_0 & 1 & k_0 & 0 \\ 0 & 0 & 1 & 0 \\ k_0 & 0 & -k_0 & 1 \end{pmatrix}. \quad (8)$$

Thus we can write the one-turn matrix of the two beams including a single beam-beam interaction :

$$\begin{pmatrix} x_{1,k+1} \\ x'_{1,k+1} \\ x_{2,k+1} \\ x'_{2,k+1} \end{pmatrix} = M_{\text{BB}} \cdot M_{2B} \cdot \begin{pmatrix} x_{1,k} \\ x'_{1,k} \\ x_{2,k} \\ x'_{2,k} \end{pmatrix}. \quad (9)$$

The normal mode analysis reveals two frequencies each corresponding to two degenerate modes. The first mode corresponds to in-phase oscillation of the two beams ( $\sigma$ -mode), its coherent tune is the unperturbed machine tune  $Q_\sigma = Q$ . The second mode of oscillation corresponds to out-of-phase oscillation of the two beams ( $\pi$ -mode), we have :

$$\cos(2\pi Q_\pi) = \cos(2\pi Q) - \beta^* k_0 \sin(2\pi Q). \quad (10)$$

The stability of the beam-beam modes is given by the imaginary part of the eigenvalues of the matrix given by Eq. (9), which is reported in Fig. 1. Comparing to Eq. (10), we see that the stability boundary is given by the resonance condition  $2Q_\pi = n$ . Since we have limited our description of the lattice and of the beam-beam interactions to first order, only the lowest order resonances are visible. In principle higher order resonances could also drive the coherent beam-beam modes [6]. It is therefore important to make sure there exist damping mechanisms for these modes, the description of which will be discussed when extending beyond the linearised model.

### The circulant matrix model

The circulant matrix model [7–9] offers a convenient way to describe the transverse oscillation of the two beams, including not only the effect of beam-beam interactions, but

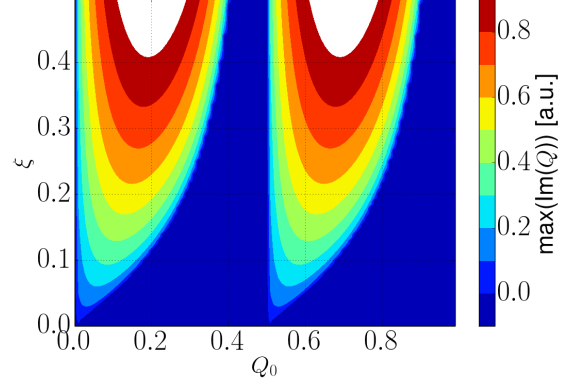


Figure 1: Largest imaginary part of the eigenvalues of Eq. (9), defining the stable area in terms of unperturbed tune  $Q_0$  and beam-beam parameter  $\xi$ .

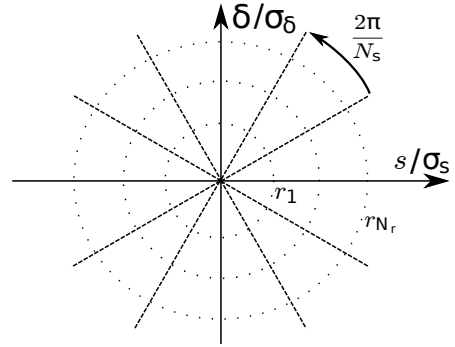


Figure 2: Discretisation of the longitudinal phase space into  $N_s$  slices and  $N_r$  rings.

also other important components of the coherent dynamic of the beam, in particular the effect of the transverse wake fields. This model is an extension of the rigid bunch model, allowing for different parts of the longitudinal phase space to oscillate independently, thus enabling the description of head-tail modes. The longitudinal phase space is discretised in polar coordinates using so-called slices and rings as illustrated in Fig. 2. The transverse motion of each discrete element can be treated as in the rigid bunch model, except that all the combinations of beam-beam interactions between the elements needs to be considered. Equation (6) becomes :

$$\Delta x_i = k_0 \left( \frac{\sum_{j=0}^{N_s N_r} Q_j x_j}{\sum_{j=0}^{N_s N_r} Q_j} - x_i \right). \quad (11)$$

As an example, let us use two slices and a single ring and start from Eq. (9) :

$$\begin{pmatrix} x_{1,1,k+1} \\ x'_{1,1,k+1} \\ x_{1,2,k+1} \\ x'_{1,2,k+1} \\ x_{2,1,k+1} \\ x'_{2,1,k+1} \\ x_{2,2,k+1} \\ x'_{2,2,k+1} \end{pmatrix} = M_{\text{BB}} \cdot M_{2B} \cdot \begin{pmatrix} x_{1,1,k} \\ x'_{1,1,k} \\ x_{1,2,k} \\ x'_{1,2,k} \\ x_{2,1,k} \\ x'_{2,1,k} \\ x_{2,2,k} \\ x'_{2,2,k} \end{pmatrix}, \quad (12)$$

where  $x_{i,j,k}$  refer to the position of slice  $j$  from beam  $i$  at turn  $k$ . The lattice matrix  $M_{2B}$  can easily be extended since all slices go through the same lattice and the beam-beam coupling matrix becomes :

$$M_{\text{BB}} = \begin{pmatrix} 1 & 0 & 0 & 0 & 0 & 0 & 0 & 0 \\ -k_0 & 1 & 0 & 0 & k_0/2 & 0 & k_0/2 & 0 \\ 0 & 0 & 1 & 0 & 0 & 0 & 0 & 0 \\ 0 & 0 & -k_0 & 1 & k_0/2 & 0 & k_0/2 & 0 \\ 0 & 0 & 0 & 0 & 1 & 0 & 0 & 0 \\ k_0/2 & 0 & k_0/2 & 0 & -k_0 & 1 & 0 & 0 \\ 0 & 0 & 0 & 0 & 0 & 0 & 1 & 0 \\ k_0/2 & 0 & k_0/2 & 0 & 0 & 0 & -k_0 & 1 \end{pmatrix}. \quad (13)$$

Such a matrix can be built in a systematic way for an arbitrary number of slices and rings, and for complex configurations of beam-beam interactions involving multiple bunches and multiple interaction points, including the longitudinal variations of the beam-beam force due to a crossing angle or to the variation of the  $\beta$  function over the interaction [10]. In order to introduce the effect of the wake, we need to take

$$M_Z = \begin{pmatrix} 1 & 0 & 0 & 0 & 0 & 0 & 0 & 0 & 0 \\ W_{\text{quad}}(s_1 - s_0) & 1 & W_{\text{dip}}(s_1 - s_0) & 0 & 0 & 0 & 0 & 0 & 0 \\ 0 & 0 & 1 & 0 & 0 & 0 & 0 & 0 & 0 \\ W_{\text{dip}}(s_0 - s_1) & 0 & W_{\text{quad}}(s_0 - s_1) & 1 & 0 & 0 & 0 & 0 & 0 \\ 0 & 0 & 0 & 0 & 1 & 0 & 0 & 0 & 0 \\ 0 & 0 & 0 & 0 & 0 & W_{\text{quad}}(s_1 - s_0) & 1 & W_{\text{dip}}(s_1 - s_0) & 0 \\ 0 & 0 & 0 & 0 & 0 & 0 & 0 & 1 & 0 \\ 0 & 0 & 0 & 0 & 0 & W_{\text{dip}}(s_0 - s_1) & 0 & W_{\text{quad}}(s_0 - s_1) & 1 \end{pmatrix}, \quad (17)$$

such that the equation of motion becomes :

$$\begin{pmatrix} x_{1,1,k+1} \\ x'_{1,1,k+1} \\ x_{1,2,k+1} \\ x'_{1,2,k+1} \\ x_{2,1,k+1} \\ x'_{2,1,k+1} \\ x_{2,2,k+1} \\ x'_{2,2,k+1} \end{pmatrix} = M_Z \cdot M_{\text{BB}} \cdot M_{2B} \cdot \begin{pmatrix} x_{1,1,k} \\ x'_{1,1,k} \\ x_{1,2,k} \\ x'_{1,2,k} \\ x_{2,1,k} \\ x'_{2,1,k} \\ x_{2,2,k} \\ x'_{2,2,k} \end{pmatrix}. \quad (18)$$

We have written the transverse one-turn matrix for the longitudinal distribution, yet the longitudinal motion has been

a closer look at the discretisation of the longitudinal phase space, in particular the longitudinal position of the discrete elements needs to be defined. The definition of the discretisation is somewhat arbitrary, however it is convenient to split the phase space such that the charge contained in each element is identical, as was implicitly assumed when deriving Eq. (13). For a Gaussian distribution of particles, the slices are uniformly distributed, we have  $\theta_i = 2\pi i/N_s$  and the radius of the rings set such that :

$$e^{-r_{j+1}} - e^{-r_j} = \frac{1}{N_r}, \quad (14)$$

where  $r_j = \sqrt{(s_j/\sigma_s)^2 + (\delta_j/\sigma_\delta)^2}$  is the radius of the  $j^{\text{th}}$  ring in the normalised longitudinal phase space, i.e.  $\sigma_s$  and  $\sigma_\delta$  are the bunch length and relative momentum spread. Therefore we obtain the longitudinal position  $s_{i,j}$  and momentum deviations  $\delta_{i,j}$  of the  $i^{\text{th}}$  slice and  $j^{\text{th}}$  ring :

$$\begin{cases} s_{i,j} &= r_j \sigma_s \cos \theta_i \\ \delta_{i,j} &= r_j \sigma_\delta \sin \theta_i \end{cases}. \quad (15)$$

Thus we can write the interaction between the discrete elements of the distribution through the beam coupling by using the integrated dipolar and quadrupolar wake functions  $W_{\text{dip}}(\Delta s)$  and  $W_{\text{quad}}(\Delta s)$  [11]:

$$\Delta x'_i = \sum_{j=0}^{N_s N_r} W_{\text{dip}}(s_j - s_i) x_j + W_{\text{quad}}(s_j - s_i) x_i. \quad (16)$$

This can be written in a matrix form, in our two-slice model and assuming that the two beams experience identical impedances, we have :

put aside. Thanks to the choice of decomposition of the longitudinal phase space, the longitudinal motion can be introduced rather simply, as it consists of a rotation of the slices within each ring. The longitudinal one-turn matrix is given by the circulant matrix :

$$S_r = P_{N_s}^{N_s Q_s}, \quad (19)$$

where  $Q_s$  is the synchrotron tune and  $P_{N_s}$  is a permutation matrix :

$$P_{N_s} = \begin{pmatrix} 0 & 1 & & & \\ & 0 & 1 & & \\ & & \ddots & \ddots & \\ 1 & & & 0 & 1 \end{pmatrix}. \quad (20)$$

Since the rotation is identical for all rings and for both beams and considering  $N_{B1}$  and  $N_{B2}$  number of bunches in the two beams, the matrix in the same basis can be built using the outer product with identity matrices :

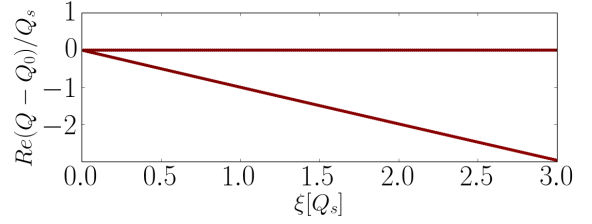
$$M_s = \mathbb{I}_{N_{B1}+N_{B2}} \otimes \mathbb{I}_{N_r} \otimes S_r. \quad (21)$$

The full one-turn matrix, including the synchro-betatron motion, the beam coupling and beam-beam interactions is then given by :

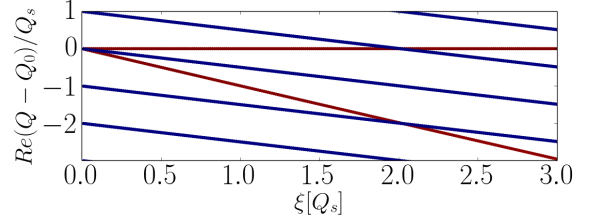
$$M = M_Z \cdot M_{BB} \cdot M_s \otimes M_{1B}, \quad (22)$$

and its stability can be studied through normal mode analysis. Let us discuss a simple configuration of two identical bunches colliding at a single interaction point without crossing angle or variations of the  $\beta$  function over the interaction length and assuming that the lattice and the impedance experienced by both beams are identical. Figure 3a shows the frequency of the two normal modes obtained with a single slice and a single ring. As expected, we find back the solution of the rigid bunch model, where the  $\sigma$ -mode frequency stays unperturbed, while the  $\pi$ -mode frequency is shifted by  $-\xi$ . Figure 3b shows the same result with a single ring and 10 slices, allowing to see the frequency of azimuthal modes, appearing as sidebands of the betatron tune. Their frequencies are shifted by  $-\xi/2$  due to the beam-beam interaction. This difference between the behaviour of the sidebands can be understood by looking at Eq. (11), where we observe that the sum over the positions of the slices is actually the dipolar moment of the oscillation. Since only the azimuthal mode 0 has a dipolar component, the other modes are only affected by the beam-beam interaction in an incoherent way. In other words, the frequency of the modes are shifted, however the corresponding sidebands of the two beams do not oscillate coherently. In the presence of wake fields, the situation is different, since the perturbed azimuthal modes may also have a dipolar component. Figure 4a illustrates the impact of a resistive wall impedance on the frequency of the normal mode in the same configuration. The perturbed modes have indeed acquired a dipolar moment, which allows them to interact through the beam-beam interaction. This effect manifests strongly as a mode coupling instability where the frequency of the  $\pi$ -mode reaches the one of the azimuthal mode -1 and where the frequency of the azimuthal mode 1 reaches the one of the  $\sigma$ -mode.

Moving towards more realistic configurations, the chromaticity also perturbs the head-tail modes, allowing them to couple through the beam-beam force at any beam-beam parameter, as shown by Fig. 4b. From this plot it is clear



(a) 1 ring, 1 slice



(b) 1 ring, 10 slices

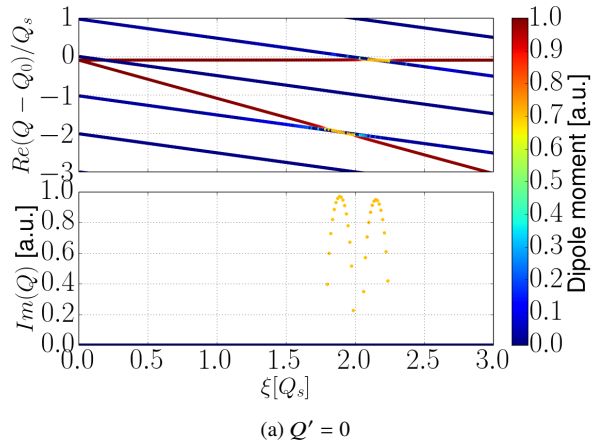
Figure 3: Eigenfrequencies of the coherent mode of oscillation of two round symmetric beams colliding head-on in one single interaction point for different beam-beam parameters. The points are colour coded according to their dipole moment, the  $\sigma$  and  $\pi$  modes are purely dipolar (red), while the synchrotron sidebands have no dipolar moment (blue). The eigenvalues are all real in absence of other mechanisms.

that an efficient damping mechanism is needed in order to maintain the stability of colliding beams. This point will be further discussed in the next section.

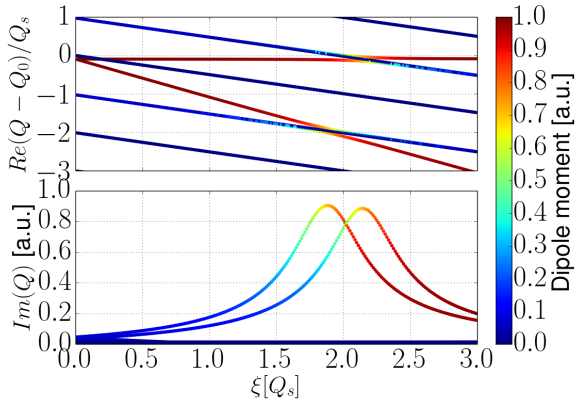
By construction the circulant matrix is well suited to study any linearised transverse force depending on the longitudinal position, such as the effect of an RF-quadrupole [12] or chromaticities of any order. The effect of a transverse feedback may also be considered [7].

As the model is based on the construction of a one-turn matrix, the modelling of multiturn effects, e.g. due to a long-range impedance source, is implicitly neglected. This limitation may be overcome by extending Eq. (16) such that the effect of previous turns is taken into account, assuming a given phase relation between the motion of the discretised element turn after turn. In other words, such a model would be based on an ad-hoc assumption on the mode of oscillation, which is not necessarily valid in complex configurations of beam-beam interactions.

Considering the one-turn matrix of multiple consecutive bunches in a given lattice, it is clear that it has several degenerate eigenvalues since every bunch has the same tune. The normal mode analysis of such a non-normal matrix is known to fail to describe its long term behaviour [13]. In accelerators, such effects were already observed as the beam breakup instability in a linear accelerator. Conceptually, the configuration of multiple bunches in a ring with a negligible multiturn wake is analogous to a linear accelerator. For



(a)  $Q' = 0$



(b)  $Q' = 2$

Figure 4: Eigenfrequencies of the coherent mode of oscillation of two round symmetric beams colliding head-on in one single interaction point for different beam-beam parameters in the presence of a resistive-wall type of impedance. In absence of chromaticity, a coupling instability appears when the frequencies of the coherent beam-beam modes reach the ones of the synchrotron sidebands. In the presence of chromaticity, the coherent interaction between the two beams has an impact on the stability of head-tail modes, at any beam-beam parameter.

example a short train of bunches in the LHC matches these assumptions, the circulant matrix model allows for a proper description of its behaviour, nevertheless the tools needed to analyse the stability of the one-turn matrix have to be adapted [10].

A major limitation of the circulant matrix lies in the linearisation of the forces which results in an inaccuracy of the frequency of the coherent modes [14] and prevents the study of transverse Landau damping.

## BEYOND THE LINEARISED MODEL

Going beyond the linearised model is crucial to understand Landau damping. Analytically, this can be achieved by

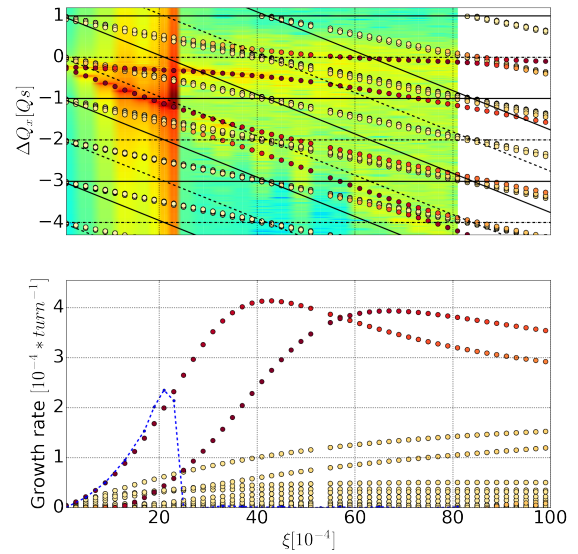


Figure 5: Estimation of the coherent modes of oscillation with the circulant matrix model using the code BimBim [10] for the nominal HL-LHC configuration [15] with a single interaction point based on the wake field of the HL-LHC model at top energy [16], which is largely dominated by the resistive wall impedance of the collimators. The dots are color coded with the dipolar component of the corresponding mode from yellow (min) to red (max). The spectrogram of the oscillation obtained with the macroparticle simulations (COMBI) is shown in the background of the upper plot, together with the exponential fit of the growth rate as a blue line in the lower plot. The dark lines represent the extension of the incoherent spectrum and its synchrotron side bands. Courtesy [17].

relaxing the constraint of the rigid bunch model and instead write the equation of motion of the particle distribution of both beams in a coupled system of Vlasov equations. Such a derivation can be found in [18], showing that in the simple configuration studied in the previous section of two identical beams colliding in a single interaction point, no Landau damping is expected for neither the  $\sigma$  nor the  $\pi$  modes due to the shift of the frequency of oscillation of the single particles due to the non-linearity of the beam-beam force, constituting the so-called incoherent spectrum. The same model predicts qualitatively Landau damping for beam-beam tune shifts exceeding the synchrotron tune, due to an interplay of the coherent beam-beam modes with the synchrotron side bands of the incoherent spectrum. In order to quantify the strength of the Landau damping in the presence of a given impedance, self-consistent macro-particle simulations need to be performed. As an example, the result of an analysis of the stability of the two beams in the HL-LHC using the code COMBI [10] is shown in Fig. 5, using a 6 dimensional model

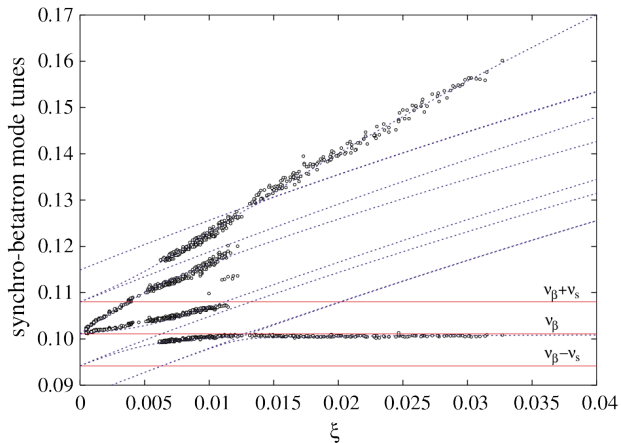


Figure 6: Measured (circles) and computed (lines) synchro-betatron coherent beam-beam mode tunes as a function of the beam-beam parameter  $\xi$  at BINP's VEPP-2M, with  $Q_x = 0.101$ ,  $Q_s = 0.0069$ ,  $\beta^* = 6$  cm,  $\sigma_s = 0.7 \cdot \beta^*$  and a beam energy of 440 MeV. Courtesy [19].

of the coherent kick taking into account the variation of the  $\beta$  function along the interaction length, the so-called hourglass effect [17]. Similarly to the chromaticity, the hourglass effect allows the beam-beam mode to couple and generate an instability at any beam-beam parameter, as shown by the prediction of the circulant matrix. As long as the frequencies of the coherent modes lie outside of the incoherent spectrum as well as its synchrotron side bands, the macro-particle simulations are consistent with the linearised model. As the  $\pi$ -mode frequency enters the lower sideband and the upper sideband overlaps with the  $\sigma$ -mode frequency, the instability predicted in the linearised model vanishes in the full model as predicted qualitatively by Vlasov perturbation theory. The remaining instability at low beam-beam parameter may be stabilised for example with a transverse feedback [9].

## OBSERVATIONS

### VEPP-2000

In absence of beam instabilities, the frequency of the head-tail coherent modes, or synchro-betatron coherent beam-beam modes, may still be investigated by exciting the beam and measuring its response in the frequency domain. This was tested at the VEPP-2M with a remarkable agreement between the circulant matrix model and the measurement (Fig. 6). Worth noting that since VEPP-2M is an electron-positron collider, the tune shift due to the beam-beam interaction is positive as opposed to the other examples discussed here from the (HL-)LHC which collides particles of identical charge.

### LHC

As opposed to BINP's VEPP-2M, CERN's LHC features a strong impedance mainly due to the collimation system, which may excite the coherent beam-beam modes. A short

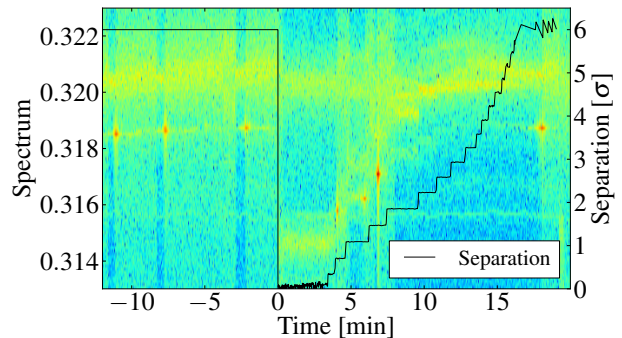


Figure 7: Spectrogram of the transverse beam oscillation during an experiment with two bunches per beam colliding with a varying transverse offset at the interaction point. The normalised separation between the beams at the IP (black line) is deduced from the measured luminosity reduction factor.

experiment was dedicated to the measurement of coupling instability with beams colliding with a transverse offset, at the end of a special fill with two bunches per beam [9]. Before  $t = 0$ , in Fig. 7, a series of spikes in the oscillation amplitude mark a few tests of the stability of separated beams without transverse feedback, by switching it off and on again when an instability was observed. At  $t = 0$ , the beams were brought into collision at one interaction point with the transverse feedback on. Once the beams were colliding HO, the transverse feedback was no longer required to maintain the beams stability. The beams were then re-separated transversally in steps, visible in Fig. 7. At each step, the stability without transverse feedback was tested, as previously. It was observed that the beams are stable without transverse feedback for separations below  $0.7 \sigma$  and from  $1.8$  to  $6 \sigma$ , whereas unstable from  $0.7$  to  $1.8 \sigma$  and at  $6 \sigma$ . Also, the instability at intermediate separations has different characteristics than for  $6 \sigma$  separation. The frequency of the mode with separated beams is consistent with a head-tail mode with  $n_a = -1$ , whereas the frequencies of the modes with intermediate separations are consistent with the ones of coherent beam-beam modes. Also, at intermediate separations both beams are unstable simultaneously, whereas at large separations, only one of the beams experienced instabilities. The small range of separations, and therefore of beam-beam tune shifts, are consistent with the circulant matrix model prediction, as well as the capacity of the transverse feedback to maintain the beam stability for any separation.

## ACKNOWLEDGEMENT

I would like to thank L. Barraud, W. Herr, K. Li, A. Mailard, T. Pieloni, M. Schenk and S.M. White for their important contributions to this topic as well as for several fruitful discussions, as well as E. Métral for both the interesting discussions and for proofreading this document.

## REFERENCES

- [1] X. Buffat et al. “Stability diagrams of colliding beams in the Large Hadron Collider.” In: *Phys. Rev. ST Accel. Beams* 17 (11 Nov. 2014), p. 111002.
- [2] C. Tambasco. “Beam Transfer Function (BTF) measurements and transverse stability in presence of beam-beam.” In: *these proceedings*. 2017.
- [3] W. Herr. “Beam-beam interactions.” In: *CAS - CERN Accelerator School: Intermediate Course on Accelerator Physics*. Ed. by D. Brandt. Zeuthen, Germany: CERN, 15-26 September 2003 2006, pp. 379–410.
- [4] M. Bassetti and G.A. Erskine. *Closed expression for the electrical field of a two-dimensional Gaussian charge*. Tech. rep. CERN-ISR-TH-80-06. Geneva: CERN, 1980.
- [5] K. Hirata. “Coherent betatron oscillation modes due to beam-beam interaction.” In: *Nucl. Instrum. Methods Phys. Res. A* 269.1 (1988), pp. 7–22. issn: 0168-9002.
- [6] Chao Alex. *Coherent Beam-Beam Effects*. Tech. rep. SSCL-346. Dallas: Superconducting Super Collider Laboratory, 1991.
- [7] V.V. Danilov and E.A. Perevedentsev. “Feedback system for the elimination of the transverse mode coupling instability.” In: *Nucl. Instrum. Methods Phys. Res. A* 391 (1997), pp. 77–92.
- [8] E. A. Perevedentsev and A. A. Valishev. “Simulation of the head-tail instability of colliding bunches.” In: *Phys. Rev. ST Accel. Beams* 4 (2 Feb. 2001), p. 024403.
- [9] S. White et al. “Transverse mode coupling instability of colliding beams.” In: *Phys. Rev. ST Accel. Beams* 17 (4 Apr. 2014), p. 041002.
- [10] X. Buffat. “Transverse beams instability studies at the Large Hadron Collider.” PhD thesis. EPFL, 2015.
- [11] B. W. Zotter and S. A. Kheifets. *Impedances and wakes in high-energy particle accelerators*. Singapore: World Scientific, 1998.
- [12] M. Schenk et al. “Analysis of transverse beam stabilization with radio frequency quadrupoles.” In: *Phys. Rev. Accel. Beams* 20 (10 Oct. 2017), p. 104402.
- [13] L. N. Trefethen and M. Embree. *Spectra and pseudospectra: The behavior of nonnormal matrices and operators*. Princeton: Princeton University Press, 2005.
- [14] K. Yokoya and H. Koiso. “Tune shift of coherent beam-beam oscillations.” In: *Part. Acc.* 27 (1990), pp. 181–186.
- [15] E. Métral et al. *Update of the HL-LHC operational scenarios for proton operation*. Tech. rep. CERN-ACC-NOTE-2018-0002. Geneva, Switzerland: CERN, Jan. 2018.
- [16] *CERN impedance webpage*. <http://impedance.web.cern.ch/impedance/>. Accessed: 2018-02-22.
- [17] Laurent Barrand and Xavier Buffat. *Mode coupling instability of colliding beams in the HL-LHC*. Tech. rep. Geneva: CERN, 2018.
- [18] Y. Alexahin. “A study of the coherent beam-beam effect in the framework of Vlasov perturbation theory.” In: *Nucl. Instrum. Methods Phys. Res. A* 480.2 (2002), pp. 253–288.
- [19] I. N. Nesterenko, E. A. Perevedentsev, and A. A. Valishev. “Coherent synchrotron beam-beam modes: Experiment and simulation.” In: *Phys. Rev. E* 65 (5 May 2002), p. 056502.